# Scaling up IL glutamatergic outputs to the amygdala alleviates opioid induced hyperalgesia in male rats

**Lingling Cui**
Tongji Hospital of Tongji Medical College of Huazhong University of Science and Technology
**Xixi Wang**
Tongji Hospital of Tongji Medical College of Huazhong University of Science and Technology
**Pengfei Zhu**
Tongji Hospital of Tongji Medical College of Huazhong University of Science and Technology
**Fang Luo**
Tongji Hospital of Tongji Medical College of Huazhong University of Science and Technology
**Chenhong Li** ( lichen@mail.scuec.edu.cn )
South-Central University for Nationalities: South-Central Minzu University

**Research Article**

**Keywords:** Opioid-induced hyperalgesia, infralimbic medial prefrontal cortex (IL), the amygdala, Neural circuits, Optogenetics, Chemogenetics

**Posted Date:** May 16th, 2023

**DOI:** https://doi.org/10.21203/rs.3.rs-2901486/v1

# Abstract

Opioids are the frontline analgesics for managing various types of pain. Paradoxically, repeated use of opioid analgesics may cause an exacerbated pain state known as opioid-induced hyperalgesia (OIH), which hinders effective clinical intervention for sever pain. Although the cellular and molecular mechanisms for OIH have been tested at different level on the pain pathway, little is known about the neural circuits underlying OIH modulation. Previous studies suggest that laterocapsular division of the central nucleus of amygdala (CeLC) is critically involved in the regulation of OIH. The purpose of this study is to clarify the role of the projections from infralimbic medial cortex (IL) to CeLC in OIH modulation. OIH was produced by repeated fentanyl subcutaneous injection in male rats. Immunofluorescence staining revealed that c-Fos-positive neurons were significantly more in the right CeLC in OIH rats than untreated rats. Then, we reported that there were functional projections from glutamate pyramidal neurons in IL to the CeLC and found that IL glutamate release onto CeLC increased after fentanyl administration. However, optogenetic activation of this IL-CeLC circuit prevented OIH by inhibiting the CeLC, while silencing this circuit by chemogenetics exacerbated OIH through activating the CeLC. Combined with the electrophysiology results, the enhanced glutamate release from IL to CeLC was a protective response rather than a reason for OIH generation. We imply that increased glutamate release was a cortical gain of IL to relieve OIH, scaling up IL outputs to CeLC may be an effective neuromodulation strategy to inhibit OIH.


# Introduction

Opioids are still the milestone analgesics for modern anesthesia and pain management [1, 2]. However, numerous studies from animals and humans showed that stronger or long-term exposure to opioid analgesics might induce a paradoxical increase in pain called opioid-induced hyperalgesia (OIH) [3–6]. Unlike Opioids tolerance, further opioid prescribing is largely futile for OIH. Compared to females and healthy males, male patients are more likely to be hyperalgesia after a bolus of fentanyl, which is among the most used opioids in clinic practice owing to its potent, relativistic long-acting analgesic action [7, 8].

The mechanisms of OIH are complicated and still being elucidated. Several hypotheses have been identified including neuroinflammation in the spinal cord and sensitization of the amygdala, as well as other cellular and molecular mechanisms in the pain matrix [9–12]. However, few studies have directly identified the neural circuits that modulate OIH.

The medial prefrontal cortex (mPFC) undergoes continuous morphological and functional changes that account for behavioral adaptations in response to pain and opioid exposure. [13–15]. As one of the important parts of the mPFC, the rat infralimbic cortex (IL) is the homolog of the human ventromedial prefrontal cortex [15–17], which regulates multiple behaviors, such as drug seeking, pain associated emotion and fear extinction [18–20]. Importantly, the IL has direct connections with the amygdala and activation of the IL- Amygdala circuit could alleviate anxiety and fear [21]. In this regard, the IL sends a dense projection to the amygdala, especially the central part of the amygdala (CeA) [22, 23]. As the main

output nucleus of the amygdala, the CeA integrates nociceptive information with multimodal information about the internal and external environment of the body [22]. Traditionally, central amygdala has divided into three areas including the central medial amygdala (CeM), the lateral central amygdala (CeL) and the capsular central amygdala (CeC) and previously, the CeC was referred to as the CeLC [24]. Our previous studies have suggested a prominent role for the CeLC in OIH development, which was activated by the high expression of ERK, CaMKIIα and mGluR1 in fentanyl-induced hyperalgesia [9, 12, 25]. In this study ,we verified the excitability of CeLC in OIH rats induced by repeated fentanyl injection with c-Fos immunostaining again. Additionally, there is evidence that the IL regulate CeLC neurons via feedforward inhibition indirectly, which is impaired in the arthritis pain model [19, 26, 27]. We hypothesized that IL modulates OIH through direct monosynaptic connections between IL and CeLC. To test this, we used in vitro patch-clamp electrophysiology with optogenetics to investigate the synaptic transmission from IL to CeLC in OIH rats. Then, we opt stimulated or chemo inhibited IL-CeLC circuit respectively to test the effects on sensory hypersensitivity after fentanyl injection. With this study we are the first to analyze the neuronal circuit mechanism of OIH. The role of IL-CeLC circuit in OIH may thus provide new reference values for future studies and for the treatment of OIH.

## Results

# 1. Fentanyl increased the activity of the right CeLC

To detect the activity of CeLC in OIH rats, we used c-Fos immunofluorescence to assess the neuronal activity after OIH was successfully established as c-Fos is a marker of neuronal activity, the timeline was shown in Fig. 1A. For basal mechanical and thermal pain threshold, there was no statistically significant difference between Saline and Fentanyl group. As shown in Fig. 1B and Fig. 1C, after subcutaneous administration of fentanyl or saline for 6.5 h, compared with the Saline group, the Fentanyl group showed significantly lower PWMT ($P$ = 0.0022, n = 6) and shorter PWTL ($P$ = 0.0029, n = 6), indicating hyperalgesia was successfully induced by fentanyl injection. We found that the level of c-Fos was significantly higher in the right CeLC region after fentanyl administration compared with the saline group (Fig. 1D, 1E, P = 0.0004, n = 6,), while on the left side, there was no significant difference between the two groups (Fig. 1F, 1G, P = 0.979, n = 6).

### 2. Monosynaptic and functional glutamate projection from IL-excitatory neurons to CeLC.

As reported, there are six cellular layers in IL, glutamate pyramidal neurons in the deep layer are responsible for sending information to other subcortical regions [35, 36]. It has been shown that calcium/calmodulin-dependent protein kinase IIα (CaMKIIα) is expressed selectively in glutamate pyramidal neurons rather than in gamma-aminobutyric acid (GABAergic) neurons in the cortex, so we use CaMKIIα to label the output-projecting pyramidal cells in the IL. [37]. To verify if CeLC neurons receive monosynaptic input from the IL, we applied 2 strategies. First, we stereotaxically inject anterograde trans-synaptic AAV1/2 carrying Cre recombinase tagged with an enhanced green fluorescent protein (EGFP) under control of CaMKIIα promoter into the IL, which can transduce axon terminals to its projecting

targets and thus was defined as “starter cells”, and then Cre-dependent DIO opsin ChR2 with CaMKIIα fused to mCherry AAV2/9 was injected into CeLC (Fig. 2A) [38, 39]. CaMKIIα is widely expressed in the CeA, so we can obtain the expression of mCherry in the CeLC [40]. 4–6 weeks later, we found that EGFP were mainly expressed in layer  of the IL (Fig. 2B), neurons with mCherry were expressed in CeLC and these are IL-projecting CeLC neurons (Fig. 2C, 2D). The overlap image indicate that the IL glutamatergic neurons could project to the CeLC neurons expressing CaMKIIα. Next, we used electrophysiology with ex vivo optogenetics to determine whether there is functional connection between IL and CeLC. As shown in Fig. 3A, we first detected the IL neurons with ChR2-EYFP can be fully activated by blue light pulses stimulation (470 nm, 20 Hz). Optostimulation (470 nm, 2 ms) of IL projecting fibers in the CeLC induced both excitatory postsynaptic currents (eEPSCs) and inhibitory postsynaptic currents (eIPSCs) (Fig. 3D). The onset latency of eEPSCs was short (Fig. 3E), indicating a monosynaptic connection between IL glutamate pyramidal neurons and CeLC. However, the latency of the eIPSCs was significantly larger than that of eEPSCs, suggesting that the inhibiting transmission were disynaptic. As shown in Fig. 3F, the light-evoked postsynaptic currents were abolished by the application of non-NMDA receptor antagonist CNQX (20 μM) and the light-evoked inhibitory postsynaptic currents (eIPSCs) could be blocked by adding $GABA_AR$ antagonist picrotoxin (PTX) (100 μM) in the ACSF. As revealed in Fig. 3G, the light-evoked postsynaptic currents (eEPSCs) were abolished by the application of tetrodotoxin (TTX, 1 μM) and recovered by 4-AP (100 μM), and then the eEPSCs were completely blocked by adding CNQX (20 μM). Further confirming the monosynaptic connection between IL glutamate neurons and the CeLC. [41, 42].

### 3. Potentiated glutamatergic inputs from IL to CeLC neurons in OIH.

To further investigate the synaptic mechanism between IL and CeLC in OIH and control rats, we explored optogenetic with patch clamp methods. We adjusted the blue light to 100% (470 nm; 2 ms) to evoke the robust response in CeLC and construct the input-output relationship of eEPSCs and eIPSCs. As revealed in Fig. 4A, cells in CeLC that were responsive to optostimulation:9/20 neurons in control rats and 9/19 neurons in OIH rats. The eIPSC/eEPSC ratio in IL-CeLC circuit didn’t have significant difference between control and OIH rats (Fig. 4B). We postulated that OIH may potentiate the glutamatergic transmission between IL and CeLC. To testify this, we evaluated the probability of presynaptic glutamate release in IL-to- CeLC connections via paired-pulse ratio (PPR) of eEPSCs, which is known to be inversely correlated with the presynaptic glutamate release. We delivered two consecutive light pulses with 100ms intervals to excite the IL afferents to get PPR (Fig. 4C). The PPR was lower in OIH rats than the saline controls, reflecting an increase of glutamate release in IL inputs to CeLC by fentanyl administration (Fig. 4D).

## 4. Activation of the IL-CeLC circuit inhibits OIH by inhibiting CeLC

To detect whether the enhanced glutamatergic projections from IL to CeLC was the cause of OIH, we activate the IL-CeLC circuit in rats by in vivo optogenetics for behavioral assessment. The timeline was shown in Fig. 4A, AAV carrying ChR2 or without ChR2 under the control of the CaMKIIα promoter (AAV2/9-CaMKIIα- ChR2-EYFP/AAV2/9- CaMKIIα-EYFP) were injected into the IL to label the output-projecting

pyramidal cells and the optic fiber was implanted just above the CeLC. (Fig. 5B). As shown in Fig. 5C, for naive rats, activation of the IL- CeLC circuit (20 Hz, 15 ms pulse, 15 mW/mm$^2$) by blue light did not affect the mechanical pain threshold (n = 7, $P$ = 0.9417;). After fentanyl injection, both groups developed hyperalgesia (Fig. 5D,5E), activation of IL inputs in rats that expressing AAV-ChR2-EYFP terminals in the CeLC notably increased both mechanical and thermal pain thresholds but did not alter the response of rats expressing only AAV-EYFP terminals. (Fig. 5D, P < 0.0001, Fig. 5E $P$< 0.0001, n = 7). As shown in Fig. 5F and Fig. 5G, compared with rats with EYFP, ChR2-mediated activation of IL-CeLC inputs decreased c-Fos expression of CeLC after fentanyl administration ($P$< 0.0001, n = 4). Taken together, optogenetically activated IL terminals in CeLC prevented OIH and decreased the activity of the CeLC. These results suggest that the increased glutamate release from IL to CeLC was not a negative thing for OIH.

# 5. Inhibition of the IL-CeLC circuit aggravates OIH by activating CeLC

To further explore the role of the IL-CeLC circuit in OIH, we decided to inhibit IL input to CeLC using Chemogenetics in *vivo*. We transfected IL with AAV encoding chemogenetic inhibitory DREADD (designer receptors exclusively activated by designer drugs) - hM4Di-EGFP and clozapine-n-oxide (CNO) can inhibit the projecting area in the CeLC exclusively [43]. As the timeline of the experiment shown in Fig. 6A, at 42 days after virus incubation, the rats were randomly divided into two groups: one group is the saline group that will be microinjected with saline into the CeLC 30 min before the behavior tests after fentanyl administration, and another group is the CNO group that will be injected with CNO at the same time with the saline group. Before fentanyl injection, the basal pain thresholds were measured to identify the hyperalgesia status. After behavior tests, all rats were sacrificed for immunostaining to confirm the location of AAV injection and cannula implantation as shown in Fig. 6B. First, we have identified chemogenetic inhibition of IL-CeLC circuit had no effect on rats without fentanyl. (Fig. 6C, n = 5, *P = 0.8518*). Then as shown in Fig. 6D and Fig. 6E, CNO could enhance both mechanical and thermal hyperalgesia after fentanyl injection (Fig. 6D, P = 0.0461, 6E, $P$ = 0.0268, n = 7). After the behavior test, immunostaining showed that inhibition of IL-CeLC circuit increased the level of c-Fos in the CeLC (Fig. 5E, 5F, P = 0.028, n = 4). These results suggested that inhibition of the IL-CeLC circuit might aggravate OIH by increasing CeLC activity. Combined with the IL-CeLC projection activation effect on OIH, the increased glutamate release from IL to CeLC might be a protective response to relieve OIH, while inhibiting this release intensified OIH.

# Discussion

As far as we know, this is the first study to focus on OIH in terms of upregulated neural circuits and validate the existence of monosynaptic glutamatergic connections between IL and CeLC in morphology using anterograde transsynaptic virus and in function by electrophysiology with optogenetics. OIH was successfully induced by fentanyl injection and an obvious activation of the right CeLC was observed. Specifically, we found that OIH caused a strengthening of glutamatergic transmission between IL and CeLC. However, Optogenetic activation of IL-CeLC circuit reversed OIH by inhibiting the CeLC, while

chemogenetic inactivation of IL-CeLC circuit exacerbate OIH by activating the CeLC, indicating that enhanced glutamate release from IL to CeLC could inhibit the activity of CeLC. Taken together, these results suggested that rather than being a cause of OIH, the change of IL glutamate neurons to CeLC might be a protective response for OIH, scaling up IL outputs to CeLC may be an effective neuromodulation strategy to inhibit OIH.

As previously reported, the pain threshold reached the lowest at 6.5 h and last almost 3days after fentanyl administration, and thus this timepoint was chosen for most of the present study [44]. As one of the immediate early genes (IEG), c-Fos would respond to extrinsic cellular stimuli and induce action potential firing and was therefore chosen as an excitatory marker [45, 46]. Interestingly, increasing evidence suggests a pain-related hemispheric lateralization in the amygdala: the right, but not left amygdala has been reported in response to inflammatory and neuropathic pain stimuli [24, 47]. Previous studies also identified the activation of ERK and mGluR1in the right but not the left CeLC after fentanyl induced hyperalgesia, which was consistent with this study. These results demonstrated that the right CeLC played a critical role in OIH [25]. Thus, the right IL-CeLC circuit was selected for behavioral tests. Also, eEPSCs and eIPSCs were recorded by whole-cell patch-clamp in the right CeLC.

As one of the primary targets for pain treatment, mPFC is widely investigated in multiple pain models, including neuropathic and inflammatory pain [41, 48–50]. Amount of data has demonstrated that projections from IL to central amygdala played a critical role in fear extinction, anxiety, and drug seeking [21, 51] but only the lateral capsular division of central nucleus of amygdala (CeLC) played a key role in modulating OIH [10, 12, 25]. Therefore, one may speculate that there are direct connections between IL and CeLC if IL can modulate OIH through amygdala. We first identified there were structural and functional connections between IL glutamate neurons and CeLC. We found that OIH potentiated glutamate release from IL to CeLC. Studies have shown that lower IL output neurons activity disrupted the feedforward inhibition to CeLC and resulted in chronic pain [19, 52]. In this study we found that activation of IL input to CeLC could inhibit the activity of CeLC and thus the CeLC-PAG-RVM-spinal cord descending facilitative pain pathway was inhibited [10]. So, we speculated that enhanced glutamate release from IL to CeLC could inhibit CeLC and thus was a positive response for OIH rats and we need more evidence to verify the proposal, which is inconsistent with the results of arthritic pain [19]. However, the activity of IL and IL-projecting CeLC neurons needs further exploration.

Prelimbic medial cortex (PL), another subregion of the medial prefrontal cortex, is next to IL anatomically, displays close functional connections with IL and has been identified to play a crucial role in chronic pain [41, 53]. Recently, we found that the oligodendrocyte decreased in the PL in OIH rats, which might affect the synaptic transmission between the PL and its projections [44]. However, there exists few projections from PL to CeLC [19]. Unlike PL, apart from pain related behaviors and emotions, IL is more associated with cue-associated behavior, such as cocaine seeking [15, 54]. Traditionally, pain is a salient sensory stimulus that elicits neural responses to protect us from injury [55]. As a kind of paradoxical pain, OIH cannot be relieved by increasing opioids. We posited that the state of hypersensitivity could be a special cue for the brain to make some changes to alleviate hyperalgesia when opioids overdosed. Therefore, this

hyperalgesia signal might activate those pain-responsive neurons in the IL as a cortical gain projecting to the CeLC to prevent OIH [48, 56]. However, this cortical gain of IL may be too weak to reverse OIH. It cannot compensate for the hyperactivity of the CeLC, so that the hyperalgesic state persists. Furthermore, scaling up this cortical gain by optogenetics completely suppressed the OIH while scaling down this cortical gain resulted in OIH aggravation.

The specific function of PFC at a given time may thus depend on the precise behavioral context and neuron function [48]. Inflammatory pain can be improved by the addition of BDNF into the IL [57], while mGluR5 in the IL might intensify nociception in arthritic rats [58]. These bidirectional functions on nociception may coincidence with each other when focus on the neuron function state. One study reported that pharmacogenetic inhibition of IL pyramidal neurons had no significant impact on pain-related wiping [30] which was consistent with our study. Activating or silencing IL-CeLC circuit did not significantly affect mechanical pain thresholds in naive rats, indicating that this cortical gain might only launch in OIH rats. Previous studies have found that the state of hyperalgesia could last for about 3 days after fentanyl administration [9, 10, 44]. However, we only select the time point for electrophysiology when the rat was most sensitive to the stimuli. This cortical gain may have been disrupted when acute pain turned into chronic pain [48, 56]. Whether this cortical gain is still existing in other timepoint needs to be explored in the future study.

Neurons in CeLC expressing CaMKIIα may play a critical role in OIH development. Our data showed that IL could modulate CeLC through glutamate transmission and we have identified some IL projection neurons in CeLC expressing CaMKIIα. One study demonstrated that optogenetic activation of CeA neurons expressing CaMKIIα-EYFP induced a transient mechanical hypersensitivity in naïve mice [59]. However, we found that activation of the IL -CeLC circuit had no effect on the pain threshold of naive rats. Another study showed that paclitaxel-induced pain activates CaMKII neurons in the amygdala, and selective inhibition of CaMKII neurons in the amygdala alleviates this pain [60]. These results were consistent with our previous study that inhibition of CaMKIIα in the central amygdala could attenuates OIH in rats [10]. Interestingly, one study found that CeA neurons expressing CaMKIIα (CeA $^{CAM}$ neurons) that project to the lateral parabrachial nucleus (LPBN) are GABAergic and optogenetic stimulation these cells attenuated nociceptive response [61]. It is also reasonable to speculate that scaling up IL input to CeLC may alleviate OIH by activating CeA $^{CAM}$ -LPBN pathway in some extent. These findings suggested that the same cells exert different functions in different models of pain. How IL modulate OIH through CeLC $^{CAM}$ neurons needs further exploration.

Another explanation is the heterogeneity of the CeLC. CeLC contains two distinct subpopulations of GABAergic neurons that express somatostatin (SOM+) or protein kinase Cδ (PKCδ+) [62–64] and they have distinct functions in pain modulating. Activating SOM + neurons would alleviate neuropathic and inflammatory pain, while activating PKCδ + neurons might enhance pain sensitivity after formalin administration and nerve injury [65, 66]. It is not accurate to speculate the cell type by morphology and thus the cell type projections from IL to CeLC remain unclear [67, 68]. Based on electrophysiological results, most of the responding cells in the CeLC were regular spiking, while reports showed that the

distribution of these two cell types had the same electrophysiology properties [65, 66]. In physiological conditions, the PKCδ + and SOM + CeLC neurons are interconnected and repress each other to restrict the output of the amygdala [69, 70]. One study found that activation of ERK in CeA mostly occurred in PKCδ + neurons after formalin injection[59]. Our previous study also found that ERK in CeLC was upregulated in OIH rats [25]. So, we speculate that the PKCδ + neurons may induce hyperalgesia by activating ERK after fentanyl administration. Optical activation of SOM + neurons increased the inhibitory control of PKCδ + neurons [59]. we supposed that increased glutamate release from IL may activate SOM + cells and inhibit ERK upregulation by inhibiting the activity of PKC + neurons and thus recover the balance of excitation and inhibition in CeLC.

There are, however, several limitations in our study. First, although we have identified the change in presynaptic glutamate release from IL to CeLC could be a cortical gain to alleviate OIH, the molecular mechanism of the synaptic change remains unclear. Then, the projections from IL to CeLC are not very rich compared with the projections from IL to basolateral amygdala (BLA), and the activity of IL-BLA projections in OIH state is still unknown [42, 71]. Moreover, earlier studies demonstrated that the CeA inhibitory microcircuits participate in fear extinction [72]. Whether the IL projection would affect the microcircuits in the CeLC after fentanyl administration is not examined.

# Materials and Methods

Animals

Male Sprague-Dawley rats weighing 70–80 g were purchased from the Animal Laboratory of Tongji Medical College, Huazhong University of Science and Technology. These little rats were prepared for virus injection. All rats were housed 4 per plastic cage before implantation under a 12 h light/dark cycle in a temperature- and humidity-controlled animal care room with access to food and water ad libitum. All animal experiments were conducted following the National Institutes of Health guide for the care and use of laboratory animals and Ethical Issue of the International Association for the Study of Pain

Fentanyl-Induced Hyperalgesia Model

The well-established Fentanyl-Induced Hyperalgesia model that mimics the high-dose opioid treatment used in human surgeries was induced as described in detail previously [28]. Fentanyl was purchased from Yichang Humanwell Pharmaceutical Co. Ltd (China) and was injected subcutaneously at a dose of 60 μg/kg for each rat, 4 times in total, with an interval of 15 min, resulting in a total dose of 240 μg/kg. The control animals were injected with the same amount of normal saline. Additionally, all rats were 350-400g for OIH model (before fentanyl administrated).

# Virus

All virus used for this experiment were packaged and purchased from Brain VTA (Wuhan, China).

# Anterograde Tracking

To verify if CeLC neurons receive monosynaptic input from IL neurons. A cre-dependent anterograde transsynaptic AAV was injected into the IL and DIO-dependent AAV was injected into the CeLC. Rats (70-80g) were anesthetized with ketamine (50 mg/kg) and xylazine (7.5 mg/kg) and then positioned in a stereotaxic frame (RWD Life Science, Shenzhen, China). After drilling a hole in the skull for the 10-μL Hamilton syringe, 0.2 μl AAV1/2-CaMKIIα-Cre-EGFP (PT0198, $1.05*10^{13}$ genome copies/ml) was injected into the right IL (AP: +3.0 mm, ML: − 0.5 mm, DV: -4.9 mm) [19, 29] at a speed of 0.1μl/min. The needles were kept in the position for another 10 min to allow the virus to diffuse. Similarly, 0.2 μl AAV2/9-CaMKIIα-hChR2-DIO-mCherry (PT0296, $5.41*10^{12}$ genome copies/ml) was injected into the right CeLC (AP: -2.3 mm, ML: − 4.2 mm, DV: -7.5 mm) [9, 10, 25]. Six weeks after virus injection, the rats were sacrificed and the brain slices were then obtained as described below in “Histology”.

# In vivo Optogenetics

After rats(70-80g) were deeply anesthetized, 0.2 μl AAV2/9-CaMKIIα-hChR2-EYFP (PT0296, $5.41*10^{12}$ genome copies/ml) or AAV2/9-CaMKIIα-EYFP (PT0107, $5.33*10^{12}$ genome copies/ml) was injected into the right IL at a speed of 0.1μl/min [30]. The rats were allowed at least 4 weeks of recovery for virus infection and then the rats were anesthetized again for optic fibers (0.37 NA, Ø2.5 mm, Inper Ltd, China) implantation. Optic fibers were implanted into the right CeLC 0.3 mm above the DV and behavior tests were performed at least one week later. To activate excitatory terminals in the CeLC from IL, a 470 nm blue light stimulator (Inper B1-470, Inper Ltd, China) were connected to the optic fiber by an optic cable. For mechanical sensitivity assessment, the light was delivered at 20 Hz, 15 ms pulse, 15 $mW/mm^2$ mode for 15 s until the reflex happened and for thermal sensitivity assessment, the light was last for 30 s at most for each test. The interval between 2 stimulations was at least 5 min [29, 31].

# Chemogenetics

To specifically inhibit IL- CeLC, the chemogenetic technology DREADD (designer receptors exclusively activated by designer drugs) was applied. And totally 0.2 μl AAV2/9-CaMKIIα-hM4D(Gi)-EGFP (PT0296, $5.41*10^{12}$ genome copies/ml) was injected into the IL. The mutated human muscarinic receptors hM4Di can be exclusively activated by CNO and the excitatory terminals from IL in the CeLC can be inhibited [32]. After 4–5 weeks recovery, a 33-gauge stainless steel cannula (RWD Life Science, Shenzhen, China) were implanted into the right CeLC (AP: -2.3 mm, ML: − 4.2 mm, DV: -7.5 mm) and behavior tests were performed at least one week later. The CNO (0.5 Mm,0.5 μl), dissolved in sterile saline was microinjected into the CeLC at the speed of 0.1 μl/min 30min before behavior tests. After infusion, the injector was kept in the place for another five minutes for drug diffusion. For the control group, the same amount of normal saline was injected into the CeLC.

# Behavioral Assessment

Prior to behavioral testing, all rats (350-400g) were placed in the special chamber to acclimate to the experimental environment for 1 hour each day at the same time as the experiment for 3 days prior to the day of the experiment. At the experiment day the nociceptive thresholds were evaluated by mechanical

and thermal hypersensitivity 6.5 h after the last fentanyl injection according to previous reports. The rats were then randomly divided into different experimental groups. Some rats were tested before, during, and after light stimulation, while some rats were tested before and after drug administration.

# Mechanical nociceptive threshold assessment

Paw-withdrawal mechanical thresholds (PWMT) were measured with von Frey filaments (North Coast, San Jose, CA, USA). The rats were placed in a transparent plastic partition with wire mesh floors to habituate until immobility before testing. A series of calibrated filaments from 0.16 g to 26g was applied perpendicularly to the plantar surface of the left hind paw in an appropriate force for about 13s, and withdrawal or licking of the paw was defined as the positive response. The interval between two filament stimulation was at least 5 min. PWMT was determined by the “up and down” method using a Dixon nonparametric test as described previously [33].

# Thermal nociceptive latency assessment

Thermal withdrawal latency (PWTL)was determined by Hargreaves test previously [9, 10]. On the day of the measurement, the rats were lying down in a clear Plexiglas chamber on top of a glass pane quietly. The radiant thermal stimulator (BME-410C, Biomedical Engineering, Boerni Science and Technology Co., Ltd., Guangzhou, China) was adjusted to the appropriate intensity to stimulate the left hind paw plantar until the rats exhibited withdrawing or licking the paw and the time was recorded. The cutoff time was set at 30 seconds to prevent tissue damage. All rats were measured at least 3 times with an interval of 5 minutes and the average of these latencies was the PWTL.

# Histology and imaging

Rats were deeply anesthetized, and then transcardially perfused with PBS (37°C, pH 7.4), followed by ice-cold paraformaldehyde (PFA). Brains were dissected and postfixed in 4% PFA overnight at 4°C. After successive equilibration in 20% and 30% sucrose in PBS, coronal slices (30 μm) were cut with a cryostat (Leica CM1950) and stored in PBS at 4°C until immunostaining. Brain slices with IL or CeLC regions were selected according to the anatomical landmarks. For c-Fos immunostaining, brain sections were washed three times with PBS for five minutes every time. Then, the brain sections were blocked in 5% normal donkey serum solution containing 0.3% Triton X-100 for 1.5 h. After washing with PBS, the slices were incubated in the rabbit anti-c-Fos(1:500, #2250, Cell Signaling Technology)overnight at 4°C. Sections were then washed in PBS and incubated in goat anti-rabbit Cy3 (1:200, Abbkine, A22220) or Dylight 488 goat anti-rabbit (1:200, Abbkine, A23220). Sections were rinsed in PBS and mounted on microscope slides with Antifade Mounting Medium with DAPI (P0131, Beyotime). All the images were captured with a Nikon N2 confocal microscope and CeLC c-Fos-positive cells were counted by a blinded observer using Image J.

To verify the location of AAV transfection, the image of brain slices with EYFP and EGFP were obtained under 488nm (light) excitation and the image of mCherry was obtained under 543nm (light) excitation.

# Electrophysiological Recordings

# Slice Preparation

Rats were anesthetized and decapitated. The brains were removed rapidly and put in the ice-cold cutting solution containing (in mM) 213 sucrose, 3 KCl, 1 $NaH_2PO_4$, 0.5 $CaCl_2$, 5 $MgCl_2$, 26 $NaHCO_3$, and 10 glucose. Coronal brain slices (300 μm) containing CeLC were obtained from the right hemisphere as described previously [25] with oxygenated (95% $O_2$ and 5% $CO_2$) cutting solution at 4°C by a Vibratome (Leica VT 1000S). The slices were allowed to recover in artificial cerebrospinal fluid (ACSF) at 37°C for at least 1 hour before recording. The ACSF contained (in mM) 125 NaCl, 5 KCl, 1.2 $NaH_2PO_4$, 2.6 $CaCl_2$, 1.3 $MgCl_2$, 26 $NaHCO_3$, and 10 glucose. All chemicals were obtained from Sigma-Aldrich.

# Whole cell patch clamp recording

To verify the AAV transfection, only slices from rats that ChR2 were strictly expressed in IL are allowed to be used. Slices containing CeLC or IL was transferred to a recording chamber and continuously perfused (2 mL/min) with oxygenated ACSF. Recording pipettes (WPI, USA, 3- 5MΩ resistance) were filled with the following internal solution (in mM):145 KCl, 5 NaCl, 10 HEPES, 5 EGTA, 4 Mg-ATP, and 0.3 $Na_3$- GTP, pH was adjusted to 7.3 with KOH and osmolarity to 280 mOsm/kg with sucrose. All chemicals were obtained from Sigma-Aldrich. Data were obtained using EPC10 amplifier and patchmaster software (HEKA, Germany), filtered and sampled at 10 kHz with a dual 4-pole Bessel filter Bessel filter (Warner Instruments, Hamden, CT). All electrophysiology data analysis was done with Clampfit software (Molecular Devices, USA).

For light activation ChR2 terminals, 2 ms blue light (pE-300white; CoolLED Ltd.) was delivered through a ×40 water-immersion objective lens (Eclipse FN1; Nikon). To confirm the functionality of expressed ChR2, APs of EYFP expressing neurons in IL were recorded by whole-cell current-clamp [34]. Light evoked postsynaptic current were recorded at -70mV(eEPSCs) and 0 mV(eIPSCs) in voltage clamp mode respectively. The non-NMDA receptor antagonist CNQX (20 μM) was added to ACSF to block glutamate receptors and $GABA_A$R antagonist picrotoxin (PTX) (100 μM) was applied to block GABA receptors. Synaptic latencies of eEPSCs and eIPSCs were determined as the time interval between the onset of light stimulation and the onset of current at holding potentials of -70 and 0 mV, respectively. To examine the monosynaptic function between IL and CeLC, eEPSCs were recorded at -70mV in voltage clamp mode. Slices were perfused with sodium channel blocker TTX (1 μM) and followed by the addition of 4-aminopyridine (4-AP, 100 μM), a potassium channel blocker, to facilitate glutamate release from synaptic terminals and then CNQX (20 μM) were applied to block glutamate receptors [21]. To record the PPR, two light pulses (2 ms duration) with an interval of 100 ms were delivered to the CeLC. The PPR was calculated as the ratio of the amplitude of the second EPSC to that of the first.

# Statistical analysis

Most data were expressed as mean ± SEM., and statistical analysis was performed by GraphPad Prism 7.0 software (GraphPad Software, San Diego, CA). Two-way RM ANOVA with Sidak's multiple comparisons test was used for behavior assessment. We use One-way ANOVA followed by the Tukey's

multiple-comparison tests to analyze differences between three or more groups. The Student's t-test was used between two groups for electrophysiology and immunofluorescence experiments. Statistical significance was set at $P < 0.05$.

# List Of Abbreviations

**CaMKIIα** calcium/calmodulin-dependent protein kinase IIα

**CeA** central part of the amygdala

**CeLC** laterocapsular division of the central nucleus of amygdala

**eEPSC** evoked excitatory postsynaptic currents

**eIPSCs** evoked inhibitory postsynaptic currents

**OIH** opioid-induced hyperalgesia

**PWTL** Thermal withdrawal latency ()

**PWMT** Paw-withdrawal mechanical thresholds

**PL** Prelimbic medial cortex

**IL** infralimbic medial cortex

# Declarations

### Ethics approval and consent to participate

All animal experiments were conducted under the approval of the Animal Care and Use Committee of Tongji Hospital, Tongji Medical College of Huazhong University of Science and Technology and we strictly followed the National Institutes of Health's guide for the care and use of laboratory animals and the policies and recommendations by the International Association for the Study of Pain.

### Consent for publication

All authors Consent for publication

### Availability of data and materials

All data generated or analyzed during this study are included in this published article. Data files used for this manuscript are available via a direct and reasonable request to the corresponding author.

### Competing interests

The authors declare no competing financial interests.


### Funding

This study was supported by grants from the National Natural Science Foundation of China (grant number: 81974165, 31870771).


### Authors' contributions

CLL designed research with input from LF and LCH; CLL and WXX performed all experiments and analyze the data; CLL, ZPF and LF wrote the paper. The author(s) read and approved the final manuscript.


### Acknowledgements

Thank the Laboratory of Membrane Ion Channels and Medicine in South-Central University for Nationalities for patch-clamp recording technique approving.



### Authors' information

[1] Department of Anesthesiology, Tongji Hospital, Tongji Medical College, Huazhong University of Science and Technology, Wuhan, Hubei, China

[2]The Laboratory of Membrane Ion Channels and Medicine, Key Laboratory of Cognitive Science, State Ethnic Affairs Commission, College of Biomedical Engineering, South-Central University for Nationalities, Wuhan, Hubei, China


# References


1. Trescot AM, Datta S, Lee M, Hansen H: **Opioid pharmacology**. *Pain physician* 2008, **11**(2 Suppl):S133-153.
2. Stanley TH: **Fentanyl**. *Journal of pain and symptom management* 2005, **29**(5 Suppl):S67-71.
3. Yi P, Pryzbylkowski P: **Opioid Induced Hyperalgesia**. *Pain medicine (Malden, Mass)* 2015, **16 Suppl 1**:S32-36.
4. Minville V, Fourcade O, Girolami JP, Tack I: **Opioid-induced hyperalgesia in a mice model of orthopaedic pain: preventive effect of ketamine**. *British journal of anaesthesia* 2010, **104**(2):231-238.
5. Weber L, Yeomans DC, Tzabazis A: **Opioid-induced hyperalgesia in clinical anesthesia practice: what has remained from theoretical concepts and experimental studies?** *Current opinion in anaesthesiology* 2017, **30**(4):458-465.
6. Fletcher D, Martinez V: **Opioid-induced hyperalgesia in patients after surgery: a systematic review and a meta-analysis**. *British journal of anaesthesia* 2014, **112**(6):991-1004.
7. Comer SD, Cahill CM: **Fentanyl: Receptor pharmacology, abuse potential, and implications for treatment**. *Neuroscience and biobehavioral reviews* 2019, **106**:49-57.

8. Schug SA, Ting S: **Fentanyl Formulations in the Management of Pain: An Update**. *Drugs* 2017, **77**(7):747-763.
9. Li Z, Li C, Yin P, Wang ZJ, Luo F: **Inhibition of CaMKIIα in the Central Nucleus of Amygdala Attenuates Fentanyl-Induced Hyperalgesia in Rats**. *The Journal of pharmacology and experimental therapeutics* 2016, **359**(1):82-89.
10. Li Z, Yin P, Chen J, Jin S, Liu J, Luo F: **CaMKIIalpha may modulate fentanyl-induced hyperalgesia via a CeLC-PAG-RVM-spinal cord descending facilitative pain pathway in rats**. *PLoS One* 2017, **12**(5):e0177412.
11. Chang L, Ye F, Luo Q, Tao Y, Shu H: **Increased Hyperalgesia and Proinflammatory Cytokines in the Spinal Cord and Dorsal Root Ganglion After Surgery and/or Fentanyl Administration in Rats**. *Anesthesia and analgesia* 2018, **126**(1):289-297.
12. Bai T, Chen H, Hu W, Liu J, Lin X, Chen S, Luo F, Yang X, Chen J, Li C: **Amygdala Metabotropic Glutamate Receptor 1 Influences Synaptic Transmission to Participate in Fentanyl-Induced Hyperalgesia in Rats**. *Cellular and molecular neurobiology* 2022.
13. Seminowicz DA, Moayedi M: **The Dorsolateral Prefrontal Cortex in Acute and Chronic Pain**. *The journal of pain* 2017, **18**(9):1027-1035.
14. Kummer KK, Mitrić M, Kalpachidou T, Kress M: **The Medial Prefrontal Cortex as a Central Hub for Mental Comorbidities Associated with Chronic Pain**. *International journal of molecular sciences* 2020, **21**(10).
15. Nett KE, LaLumiere RT: **Infralimbic cortex functioning across motivated behaviors: Can the differences be reconciled?** *Neuroscience and biobehavioral reviews* 2021, **131**:704-721.
16. Delgado MR, Beer JS, Fellows LK, Huettel SA, Platt ML, Quirk GJ, Schiller D: **Viewpoints: Dialogues on the functional role of the ventromedial prefrontal cortex**. *Nature neuroscience* 2016, **19**(12):1545-1552.
17. Carlén M: **What constitutes the prefrontal cortex?** *Science (New York, NY)* 2017, **358**(6362):478-482.
18. Hurley SW, Carelli RM: **Activation of Infralimbic to Nucleus Accumbens Shell Pathway Suppresses Conditioned Aversion in Male But Not Female Rats**. *The Journal of neuroscience : the official journal of the Society for Neuroscience* 2020, **40**(36):6888-6895.
19. Kiritoshi T, Neugebauer V: **Pathway-Specific Alterations of Cortico-Amygdala Transmission in an Arthritis Pain Model**. *ACS chemical neuroscience* 2018, **9**(9):2252-2261.
20. Dulka BN, Bagatelas ED, Bress KS, Grizzell JA, Cannon MK, Whitten CJ, Cooper MA: **Chemogenetic activation of an infralimbic cortex to basolateral amygdala projection promotes resistance to acute social defeat stress**. *Scientific reports* 2020, **10**(1):6884.
21. Chen YH, Wu JL, Hu NY, Zhuang JP, Li WP, Zhang SR, Li XW, Yang JM, Gao TM: **Distinct projections from the infralimbic cortex exert opposing effects in modulating anxiety and fear**. *The Journal of clinical investigation* 2021, **131**(14).
22. Thompson JM, Neugebauer V: **Amygdala Plasticity and Pain**. *Pain research & management* 2017, **2017**:8296501.

23. Veinante P, Yalcin I, Barrot M: **The amygdala between sensation and affect: a role in pain**. *Journal of molecular psychiatry* 2013, **1**(1):9.
24. Allen HN, Bobnar HJ, Kolber BJ: **Left and right hemispheric lateralization of the amygdala in pain**. *Progress in neurobiology* 2021, **196**:101891.
25. Li Z, Yin P, Chen J, Li C, Liu J, Rambojan H, Luo F: **Activation of the Extracellular Signal-Regulated Kinase in the Amygdale Modulates Fentanyl-Induced Hypersensitivity in Rats**. *The journal of pain* 2017, **18**(2):188-199.
26. Neugebauer V: **Amygdala physiology in pain**. *Handb Behav Neurosci* 2020, **26**:101-113.
27. Neugebauer V, Mazzitelli M, Cragg B, Ji G, Navratilova E, Porreca F: **Amygdala, neuropeptides, and chronic pain-related affective behaviors**. *Neuropharmacology* 2020, **170**:108052.
28. Célèrier E, Rivat C, Jun Y, Laulin JP, Larcher A, Reynier P, Simonnet G: **Long-lasting hyperalgesia induced by fentanyl in rats: preventive effect of ketamine**. *Anesthesiology* 2000, **92**(2):465-472.
29. Liang SH, Zhao WJ, Yin JB, Chen YB, Li JN, Feng B, Lu YC, Wang J, Dong YL, Li YQ: **A Neural Circuit from Thalamic Paraventricular Nucleus to Central Amygdala for the Facilitation of Neuropathic Pain**. *The Journal of neuroscience : the official journal of the Society for Neuroscience* 2020, **40**(41):7837-7854.
30. Chen M, He T, Yi XH, Tang MC, Long JH, Wang PJ, Liu J, Yao J, Li HL, Sui JF *et al*: **Infralimbic cortex-medial striatum projections modulate the itch processing**. *Experimental neurology* 2022, **354**:114101.
31. Avegno EM, Lobell TD, Itoga CA, Baynes BB, Whitaker AM, Weera MM, Edwards S, Middleton JW, Gilpin NW: **Central Amygdala Circuits Mediate Hyperalgesia in Alcohol-Dependent Rats**. *The Journal of neuroscience : the official journal of the Society for Neuroscience* 2018, **38**(36):7761-7773.
32. Chang YT, Chen WH, Shih HC, Min MY, Shyu BC, Chen CC: **Anterior nucleus of paraventricular thalamus mediates chronic mechanical hyperalgesia**. *Pain* 2019, **160**(5):1208-1223.
33. Chaplan SR, Bach FW, Pogrel JW, Chung JM, Yaksh TL: **Quantitative assessment of tactile allodynia in the rat paw**. *Journal of neuroscience methods* 1994, **53**(1):55-63.
34. Liang HY, Chen ZJ, Xiao H, Lin YH, Hu YY, Chang L, Wu HY, Wang P, Lu W, Zhu DY *et al*: **nNOS-expressing neurons in the vmPFC transform pPVT-derived chronic pain signals into anxiety behaviors**. *Nature communications* 2020, **11**(1):2501.
35. Mitric M, Seewald A, Moschetti G, Sacerdote P, Ferraguti F, Kummer KK, Kress M: **Layer- and subregion-specific electrophysiological and morphological changes of the medial prefrontal cortex in a mouse model of neuropathic pain**. *Scientific reports* 2019, **9**(1):9479.
36. Metz AE, Yau HJ, Centeno MV, Apkarian AV, Martina M: **Morphological and functional reorganization of rat medial prefrontal cortex in neuropathic pain**. *Proceedings of the National Academy of Sciences of the United States of America* 2009, **106**(7):2423-2428.
37. Ong WY, Stohler CS, Herr DR: **Role of the Prefrontal Cortex in Pain Processing**. *Molecular neurobiology* 2019, **56**(2):1137-1166.

38. Zingg B, Dong HW, Tao HW, Zhang LI: **Application of AAV1 for Anterograde Transsynaptic Circuit Mapping and Input-Dependent Neuronal Cataloging**. *Current protocols* 2022, **2**(1):e339.
39. Zingg B, Chou XL, Zhang ZG, Mesik L, Liang F, Tao HW, Zhang LI: **AAV-Mediated Anterograde Transsynaptic Tagging: Mapping Corticocollicular Input-Defined Neural Pathways for Defense Behaviors**. *Neuron* 2017, **93**(1):33-47.
40. Wang X, Zhang C, Szábo G, Sun QQ: **Distribution of CaMKIIα expression in the brain in vivo, studied by CaMKIIα-GFP mice**. *Brain research* 2013, **1518**:9-25.
41. Huang J, Gadotti VM, Chen L, Souza IA, Huang S, Wang D, Ramakrishnan C, Deisseroth K, Zhang Z, Zamponi GW: **A neuronal circuit for activating descending modulation of neuropathic pain**. *Nature neuroscience* 2019, **22**(10):1659-1668.
42. Liu WZ, Zhang WH, Zheng ZH, Zou JX, Liu XX, Huang SH, You WJ, He Y, Zhang JY, Wang XD *et al*: **Identification of a prefrontal cortex-to-amygdala pathway for chronic stress-induced anxiety**. *Nature communications* 2020, **11**(1):2221.
43. Gomez JL, Bonaventura J, Lesniak W, Mathews WB, Sysa-Shah P, Rodriguez LA, Ellis RJ, Richie CT, Harvey BK, Dannals RF *et al*: **Chemogenetics revealed: DREADD occupancy and activation via converted clozapine**. *Science (New York, NY)* 2017, **357**(6350):503-507.
44. Wang XX, Cui LL, Gan SF, Zhang ZR, Xiao J, Li CH, Luo F: **Inhibition of Oligodendrocyte Apoptosis in the Prelimbic Medial Prefrontal Cortex Prevents Fentanyl-induced Hyperalgesia in Rats**. *The journal of pain* 2022.
45. Fields RD, Eshete F, Stevens B, Itoh K: **Action potential-dependent regulation of gene expression: temporal specificity in ca2+, cAMP-responsive element binding proteins, and mitogen-activated protein kinase signaling**. *The Journal of neuroscience : the official journal of the Society for Neuroscience* 1997, **17**(19):7252-7266.
46. Sheng HZ, Fields RD, Nelson PG: **Specific regulation of immediate early genes by patterned neuronal activity**. *Journal of neuroscience research* 1993, **35**(5):459-467.
47. Sadler KE, McQuaid NA, Cox AC, Behun MN, Trouten AM, Kolber BJ: **Divergent functions of the left and right central amygdala in visceral nociception**. *Pain* 2017, **158**(4):747-759.
48. Dale J, Zhou H, Zhang Q, Martinez E, Hu S, Liu K, Urien L, Chen Z, Wang J: **Scaling Up Cortical Control Inhibits Pain**. *Cell reports* 2018, **23**(5):1301-1313.
49. Zhang Z, Gadotti VM, Chen L, Souza IA, Stemkowski PL, Zamponi GW: **Role of Prelimbic GABAergic Circuits in Sensory and Emotional Aspects of Neuropathic Pain**. *Cell reports* 2015, **12**(5):752-759.
50. Cardoso-Cruz H, Paiva P, Monteiro C, Galhardo V: **Selective optogenetic inhibition of medial prefrontal glutamatergic neurons reverses working memory deficits induced by neuropathic pain**. *Pain* 2019, **160**(4):805-823.
51. Tao Y, Cai CY, Xian JY, Kou XL, Lin YH, Qin C, Wu HY, Chang L, Luo CX, Zhu DY: **Projections from Infralimbic Cortex to Paraventricular Thalamus Mediate Fear Extinction Retrieval**. *Neuroscience bulletin* 2021, **37**(2):229-241.

52. Kiritoshi T, Ji G, Neugebauer V: **Rescue of Impaired mGluR5-Driven Endocannabinoid Signaling Restores Prefrontal Cortical Output to Inhibit Pain in Arthritic Rats**. *The Journal of neuroscience : the official journal of the Society for Neuroscience* 2016, **36**(3):837-850.
53. Mukherjee A, Caroni P: **Infralimbic cortex is required for learning alternatives to prelimbic promoted associations through reciprocal connectivity**. *Nature communications* 2018, **9**(1):2727.
54. Caballero JP, Scarpa GB, Remage-Healey L, Moorman DE: **Differential Effects of Dorsal and Ventral Medial Prefrontal Cortex Inactivation during Natural Reward Seeking, Extinction, and Cue-Induced Reinstatement**. *eNeuro* 2019, **6**(5).
55. Basbaum AI, Bautista DM, Scherrer G, Julius D: **Cellular and molecular mechanisms of pain**. *Cell* 2009, **139**(2):267-284.
56. Li A, Liu Y, Zhang Q, Friesner I, Jee HJ, Chen ZS, Wang J: **Disrupted population coding in the prefrontal cortex underlies pain aversion**. *Cell reports* 2021, **37**(6):109978.
57. Yue L, Ma LY, Cui S, Liu FY, Yi M, Wan Y: **Brain-derived neurotrophic factor in the infralimbic cortex alleviates inflammatory pain**. *Neuroscience letters* 2017, **655**:7-13.
58. David-Pereira A, Puga S, Gonçalves S, Amorim D, Silva C, Pertovaara A, Almeida A, Pinto-Ribeiro F: **Metabotropic glutamate 5 receptor in the infralimbic cortex contributes to descending pain facilitation in healthy and arthritic animals**. *Neuroscience* 2016, **312**:108-119.
59. Chen WH, Lien CC, Chen CC: **Neuronal basis for pain-like and anxiety-like behaviors in the central nucleus of the amygdala**. *Pain* 2022, **163**(3):e463-e475.
60. Liu J, Li D, Huang J, Cao J, Cai G, Guo Y, Wang G, Zhao S, Wang X, Wu S: **Glutamatergic Neurons in the Amygdala Are Involved in Paclitaxel-Induced Pain and Anxiety**. *Frontiers in psychiatry* 2022, **13**:869544.
61. Hogri R, Teuchmann HL, Heinke B, Holzinger R, Trofimova L, Sandkühler J: **GABAergic CaMKIIα+ Amygdala Output Attenuates Pain and Modulates Emotional-Motivational Behavior via Parabrachial Inhibition**. *The Journal of neuroscience : the official journal of the Society for Neuroscience* 2022, **42**(27):5373-5388.
62. Li H, Penzo MA, Taniguchi H, Kopec CD, Huang ZJ, Li B: **Experience-dependent modification of a central amygdala fear circuit**. *Nature neuroscience* 2013, **16**(3):332-339.
63. Kim J, Zhang X, Muralidhar S, LeBlanc SA, Tonegawa S: **Basolateral to Central Amygdala Neural Circuits for Appetitive Behaviors**. *Neuron* 2017, **93**(6):1464-1479.e1465.
64. Zeng N, Cutts EJ, Lopez CB, Kaur S, Duran M, Virkus SA, Hardaway JA: **Anatomical and Functional Characterization of Central Amygdala Glucagon-Like Peptide 1 Receptor Expressing Neurons**. *Frontiers in behavioral neuroscience* 2021, **15**:724030.
65. Wilson TD, Valdivia S, Khan A, Ahn HS, Adke AP, Martinez Gonzalez S, Sugimura YK, Carrasquillo Y: **Dual and Opposing Functions of the Central Amygdala in the Modulation of Pain**. *Cell reports* 2019, **29**(2):332-346.e335.
66. Adke AP, Khan A, Ahn HS, Becker JJ, Wilson TD, Valdivia S, Sugimura YK, Martinez Gonzalez S, Carrasquillo Y: **Cell-Type Specificity of Neuronal Excitability and Morphology in the Central**

**Amygdala**. *eNeuro* 2021, **8**(1).

67. LeDoux J: **The amygdala**. *Current biology : CB* 2007, **17**(20):R868-874.
68. Sah P, Faber ES, Lopez De Armentia M, Power J: **The amygdaloid complex: anatomy and physiology**. *Physiological reviews* 2003, **83**(3):803-834.
69. Haubensak W, Kunwar PS, Cai H, Ciocchi S, Wall NR, Ponnusamy R, Biag J, Dong HW, Deisseroth K, Callaway EM *et al*: **Genetic dissection of an amygdala microcircuit that gates conditioned fear**. *Nature* 2010, **468**(7321):270-276.
70. Hunt S, Sun Y, Kucukdereli H, Klein R, Sah P: **Intrinsic Circuits in the Lateral Central Amygdala**. *eNeuro* 2017, **4**(1).
71. Marek R, Strobel C, Bredy TW, Sah P: **The amygdala and medial prefrontal cortex: partners in the fear circuit**. *The Journal of physiology* 2013, **591**(10):2381-2391.
72. Whittle N, Fadok J, MacPherson KP, Nguyen R, Botta P, Wolff SBE, Müller C, Herry C, Tovote P, Holmes A *et al*: **Central amygdala micro-circuits mediate fear extinction**. *Nature communications* 2021, **12**(1):4156.

# Figures

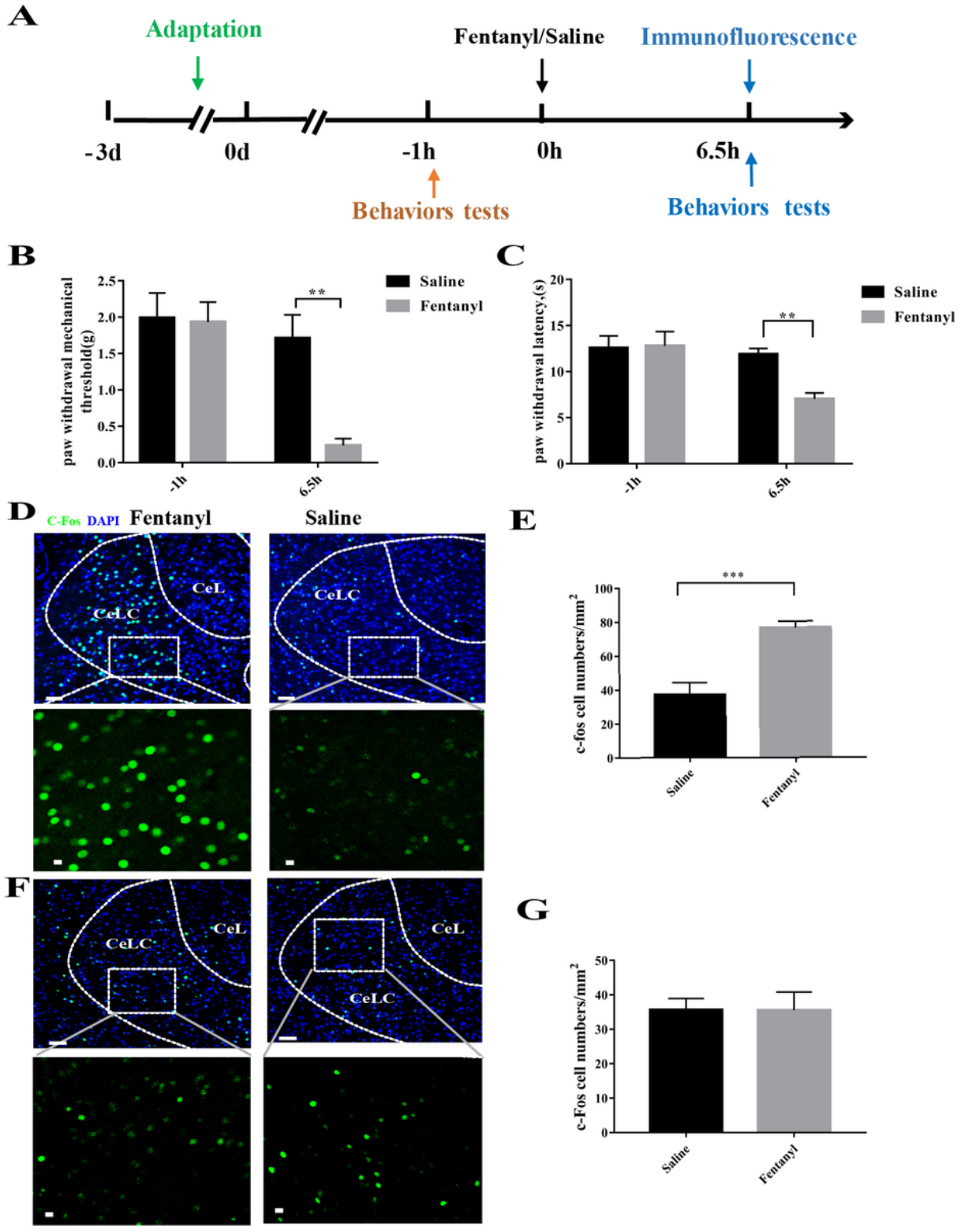


## Figure 1

Fentanyl administration increases the c-Fos expression in the right CeLC. (A) Illustration of the experimental timeline. (B, C) Repeated fentanyl injection induced mechanical [B, Finteraction(1,10) = 6.67, P = 0.0273; Ftime (1, 10) = 12.93; P = 0.0049]and thermal hypersensitivity[C, Finteraction(1,10)=6.46, P=0.0293 ; Ftime (1, 10) = 10.5; P = 0.0089] (60μg/kg, 4 times, 15-minute intervals, subcutaneous, n = 6 in each group, by two-way RM ANOVA with Sidak's multiple comparisons test). (D) Representative c-Fos

immunofluorescence images of the right CeLC (up, scale bars 100 μm) and high-magnification images (down, scale bars:50 μm) from selected areas in the up images. (E) The number of c-Fos positive neurons in the right CeLC (n = 4, P = 0.0004, unpaired t-test). (F) Representative c-Fos immunofluorescence images of the left CeLC (up, scale bars 100 mm) and high-magnification images (down, scale bars:50 mm) from selected areas in the up images. (G) Number of c-Fos positive neurons in the Left CeLC (n = 4, P = 0.979, unpaired t-test) compared with saline-injected rats. **P <0.01, ***P <0.001, data are presented as the mean ± SEM.

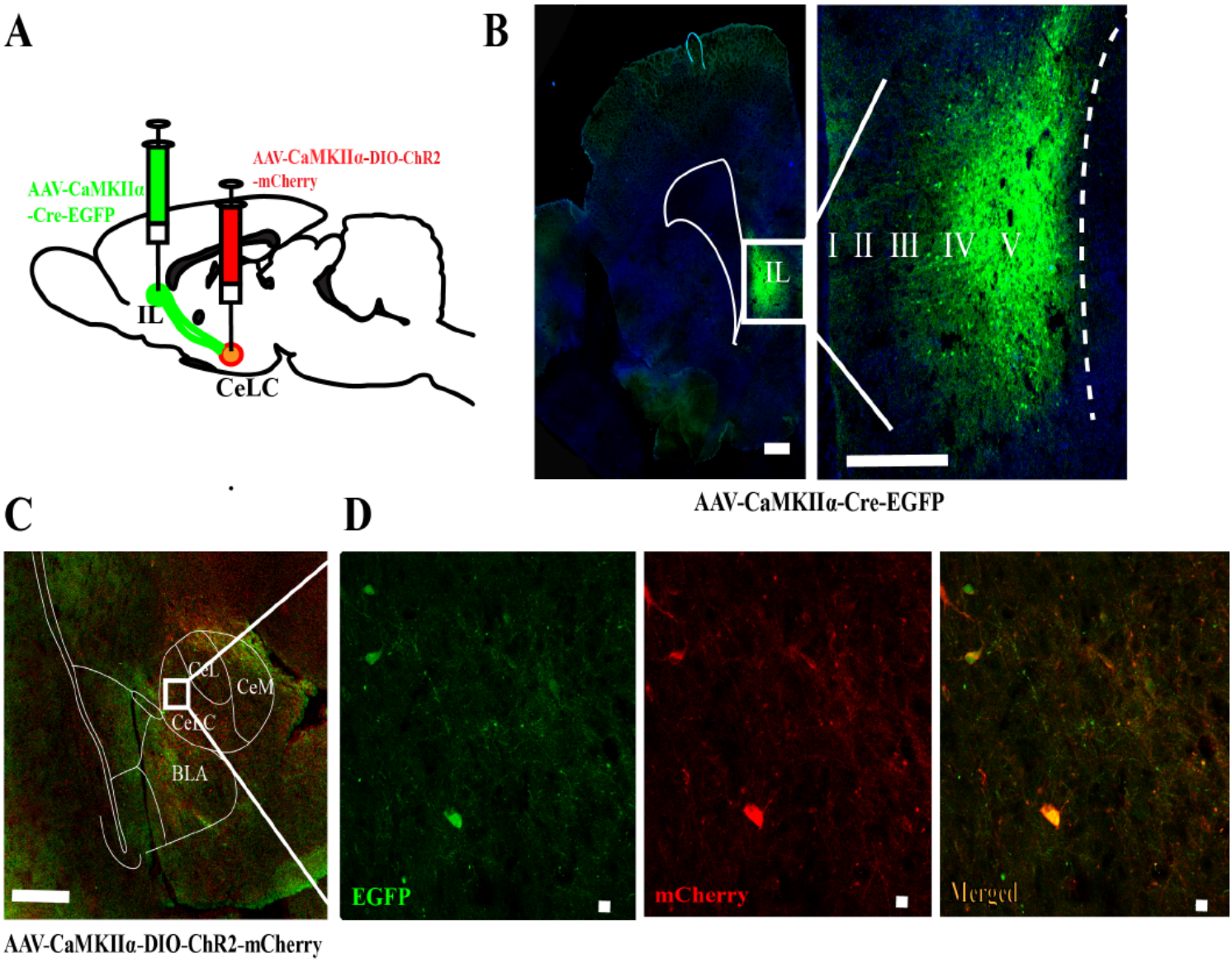


## Figure 2

**IL Glutamate projection to CeLC neurons expressing CaMKIIα.** (A) Experimental scheme: injection of AAV-Cre- EGFP into IL and AAV-DIO-ChR2-mCherry into the CeLC. (B) Fluorescence images representing the location of EGFP expression in the IL neurons. (C) mCherry expression in the CeLC neurons. (D) High-magnification images showed that IL-projecting EGFP neurons can merge with neurons expressing mCherry in CeLC. (scale bars, B, C:1000mm, D:50mm, n=3)

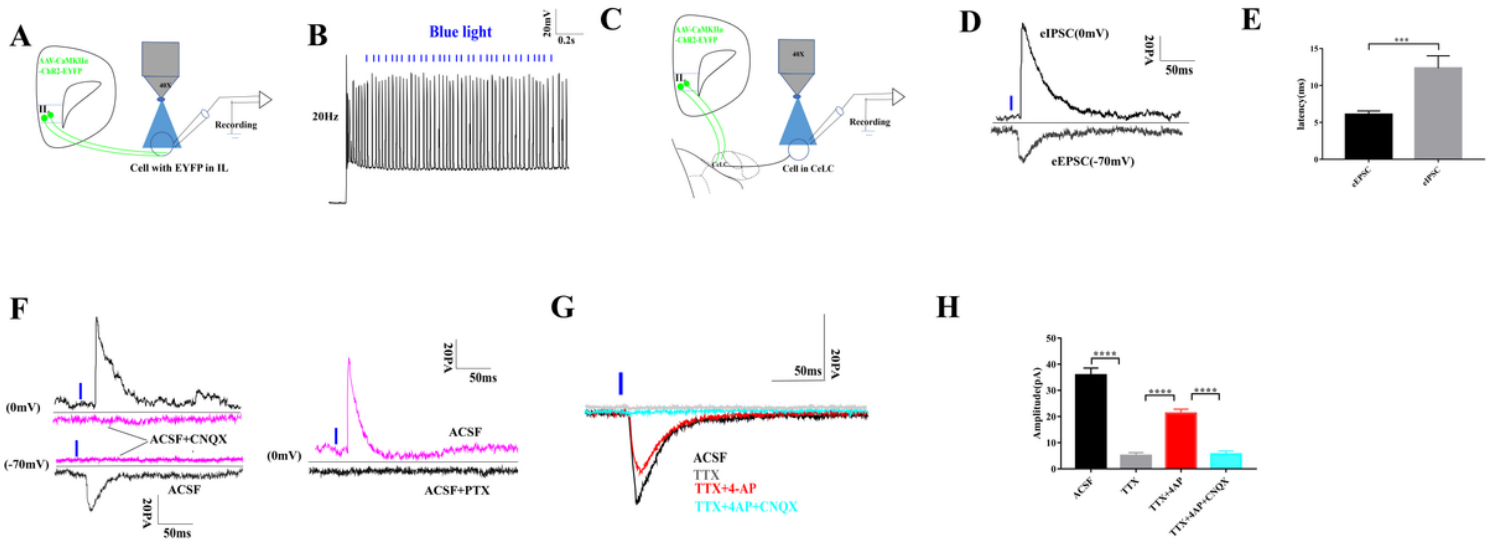


## Figure 3

**Monosynaptic functional IL glutamate inputs into the CeLC.** (A) Diagram to verify the ChR2 have the function in the IL. (B) APs were induced in pyramidal neurons expressing ChR2 in IL by 2 ms light stimulation pulses of 20Hz in current clamping mode. (C)Scheme for recording light-evoked postsynaptic currents in the CeLC by optogenetic activation of the IL projections. (D) Representative traces of IL-evoked EPSCs and IPSCs after optostimulation (blue bars, 470 nm, 2ms) in CeLC at -70 and 0 mV, respectively. (E)The latency of eIPSCs is significantly larger than that of eEPSCs. eEPSCs: n = 12 neurons /5 rats; eIPSCs: n = 9 neurons /4 rats. (F) Representative traces showing effects of 6-cyano-7-nitroquinoxaline-2,3-dioneis (CNQX, 20 μM) or picrotoxin (PTX,100 μM) on IL-evoked EPSCs/IPSCs. Cells were held at -70 and 0 mV, respectively. (G) Light-evoked postsynaptic currents were completely blocked by TTX (1 μM) and recovered by TTX plus 4-AP (100 μM), and then were blocked by CNQX (20 μM). (H) Summary plots of the eEPSCs amplitudes in (G). [G, n = 7 neurons from 3 mice, $F(3,20) = 70.31$, $P < 0.0001$; one-way ANOVA with Tukey's multiple-comparison test]. ***$P < 0.001$, ****$P < 0.0001$, Data are presented as the mean ± SEM.

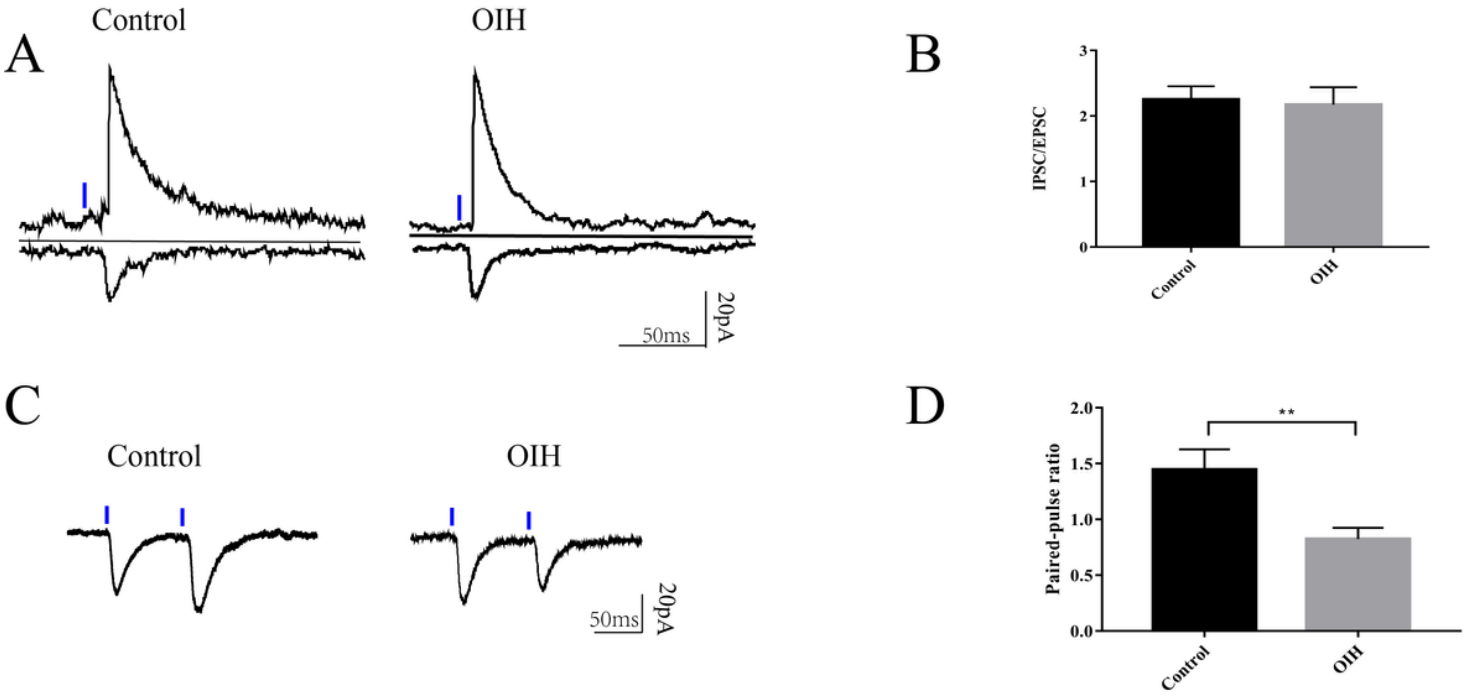


## Figure 4

**OIH increases IL glutamate release onto CeLC.** (A) Representative traces of the evoked EPSCs/IPSCs in CeLC neurons of control and OIH rats following light activation of IL inputs. (B) The eIPSC/eEPSC ratio of CeLC cells was not different between OIH and control rats. (unpaired t test, *P=0.8152,* n =9 neurons/5 rats in OIH and control rats respectively). (C) Representative traces of the paired-pulse ratio (PPR) of eEPSCs in the CeLC neurons from control and OIH rats. (D) The PPR in the CeLC neurons was lower in OIH rats than the saline controls. (unpaired t test, *P=0.0098,*n =10 neurons/5 rats in OIH rats and n = 9 neurons/5 rats in control rats respectively) ***P < 0.01,* data are presented as the mean ± SEM.

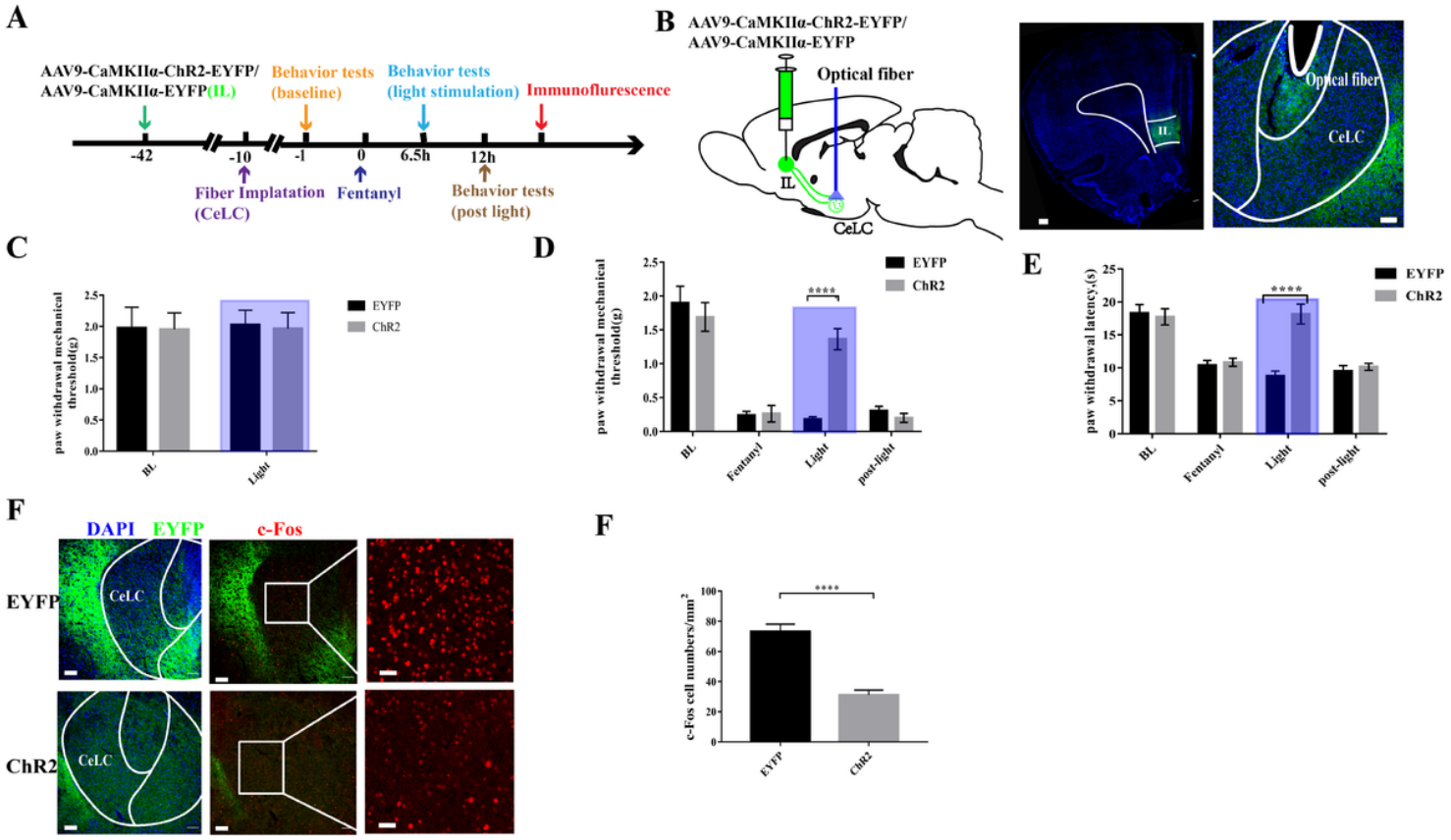


## Figure 5

**Optical stimulation of IL terminals in CeLC is sufficient to inhibit OIH and decrease the activity of CeLC** (A) Experimental paradigm for optogenetic activation: Neurons in the IL were transduced with ChR2 -EYFP or EYFP. The blue light was delivered via optical fibers implanted into the CeLC after 4-6 weeks of viral incubation. (B) Left: Schematic diagram of the location of virus injection and optical fiber implantation. Right: Fluorescence images showing AAV-EYFP expression in IL (scale bars 1000 mm) and CeLC optical fiber implantation location (scale bars 100 mm). (C) Mechanical paw withdrawal threshold when optogenetic activation of IL-CeLC circuit in naïve rats. (n = 7, $F_{interaction}$ (1, 24) = 0.0054; $P$ =0.9417) (D, E) Mechanical paw withdrawal threshold and thermal paw withdrawal latency of the ChR2 group were increased after blue light activation of IL inputs in the CeLC. [D, $F_{interaction}$ (3,36)=15.02, $P$ < 0.0001; $F_{time}$ (3, 36) = 76.11, $P$ < 0.0001 n = 7; E, $F_{interaction}$ (3,36) = 8.455, $P$ = 0.0002;$F_{time}$ (3, 36) = 20.57 , $P$ < 0.0001, n = 7, two-way RM ANOVA with Sidak's multiple comparisons test] (F) Representative c-Fos immunofluorescence images in the right CeLC after optogenetic activation of IL- CeLC circuit (scale bars: left and middle :100mm; right: 50mm ). (G) Number of c-Fos positive neurons in the right CeLC after optogenetic activation of IL- CeLC circuit (n = 4, unpaired t-test, $P$ < 0.0001) *****P < 0.0001,* data are presented as the mean ± SEM.

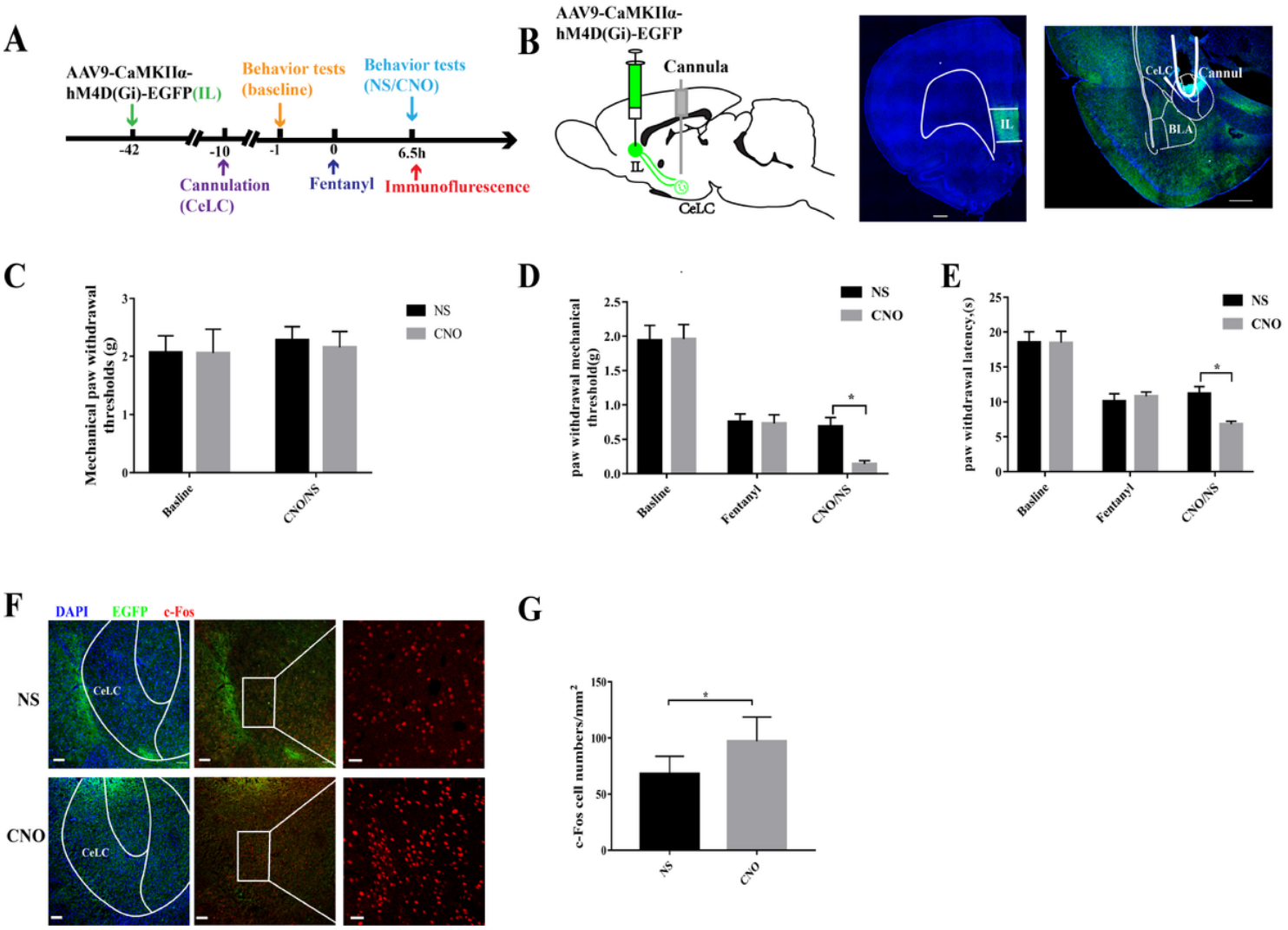


## Figure 6

**Chemogenetic inhibition of IL terminals in CeLC exacerbates OIH and increases the activity of CeLC** (A) Experimental diagram for Chemogenetic inhibition: neurons in the IL were transduced with hM4Di-EGFP, CNO or saline was delivered via a cannula implanted in the CeLC after 4-6 weeks of virus incubation. (B) Left: Schematic diagram of the location of virus injection and cannula implantation. Right: Fluorescence images showing AAV-EGFP expression in IL and CeLC cannula location (scale bars 1000 mm). (C) Mechanical paw withdrawal threshold when chemogenetic inhibition of IL-CeLC circuit in naïve rats [n = 5, $F_{interaction}$ (1, 16) = 0.03605, $P$ = 0.8518; two-way RM ANOVA with Bonferroni's multiple comparisons test]. (D, E) Mechanical paw withdrawal threshold and thermal paw withdrawal latency of the CNO group were decreased after Chemogenetic inhibition of IL inputs to the CeLC. [C: n = 7, $F_{interaction}$ (2, 24) = 2.394, $P$=0.1127; $F_{time}$ (2, 24) = 63.83, $P$ < 0.0001 D: $F_{interaction}$ (2, 24) = 2.721, $P$ = 0.0861; $F_{time}$ (2, 24) = 37.96, $P$ < 0.0001; two-way RM ANOVA with Sidak's multiple comparisons test] (F) Representative c-Fos immunofluorescence images of the right CeLC after Chemogenetic inhibition of IL- CeLC circuit ((scale bars: left and middle :100mm; right: 50mm). (G) Number of c-Fos positive neurons in the right CeLC after Chemogenetic inhibition of IL- CeLC circuit (n=4, unpaired t-test, $P$=0.028). *$P < 0.05$, data are presented as the mean ± SEM.